doi:10.1246/cl.2011.1173
Published on the web October 1, 2011

One-step Solid-state Reaction for the Synthesis of Hexagonal or Rhombohedral Boron Nitride Nanoplates in Autoclaves

Tingting Wang, Zhicheng Ju, Changhui Sun, and Yitai Qian*
Department of Chemistry, Shandong University, Jinan 250100, P. R. China

(Received April 19, 2011; CL-110325; E-mail: qianyt@sdu.edu.cn)

Crystalline hexagonal boron nitride (h-BN) hexagonal nanoplates were synthesized by the reaction of B_2O_3, NH_4F, and metallic Na at 700 °C. The edge sizes of the hexagonal nanoplates are 400 nm, and the average thickness is 100 nm. As the reaction temperature was set at 500 °C, rhombohedral boron nitride (r-BN) triangular nanoplates nearly 200 nm across and about 20 nm thick were obtained. TGA analysis results reveal that thermal stability of h-BN hexagonal nanoplates was better than that of r-BN triangular nanoplates in air.

Boron nitride (BN) has attracted great concern due to its high thermal stability, high melting point, and low dielectric constant, making it a promising lubricants, electric insulators, and refractory materials.[1,2] Typically, BN has four polymorphs: hexagonal BN (h-BN), rhombohedral BN (r-BN), wurtzite BN, and cubic BN (c-BN). Earlier reports show that the realization of the phase transformation from r-BN to h-BN occurred only at temperatures exceeding 2100 K in argon for a highly dispersed phase.[3] Recent study has shown that this transformation occurs even at 1650 K.[4] In addition, a variety of methods have been used for the synthesis of novel morphologies of h-BN or r-BN nanomaterials, for example, CVD growth of h-BN and r-BN nanotube mixtures[5] as well as r-BN and c-BN nanoparticles,[6] copyrolysis of BBr_3 and NaN_3 for the synthesis of h-BN hollow spheres,[7] sulfur-assisted synthesis of h-BN nanorings,[8] growing r-BN nanobamboo structures at 1300 °C with ammonia,[9] and low-temperature synthesis of c-BN and h-BN.[10] Although great efforts have been made toward the synthesis and wider use of BN, it is still a challenge to develop a safe and efficient route to prepare BN nanomaterials at relatively mild temperature.

The calculated results of the 2D BN structure indicated that their electronic, magnetic, and mechanical properties are excellent,[11] which enable 2D BN nanostructures to have potential applications in optoelectronic and thermoelectric devices.[12,13] Up to now, the preparation of several 2D BN nanostructures has been reported such as Ni-assisted synthesis of r-BN triangular nanoplates,[14] thermally induced synthesis of r-BN hexagonal nanoplates in flowing N_2,[15] and preparation of the h-BN nanosheets by solution exfoliation.[16] However, the synthesis of 2D BN triangular or hexagonal nanoplates with relatively uniform morphology through a solid-state route is still a challenge.

Herein, h-BN has been prepared by the reaction of B_2O_3, NH_4F, and metallic Na at 700 °C in an autoclave. It was found that the reaction temperature has a key influence on the phase and morphology of the product. As the reaction temperature was set at 500 °C, while keeping other conditions unchanged, r-BN was obtained. The overall favorable reaction could be written as follows:

$$B_2O_3 + 2NH_4F + 2Na \rightarrow 2BN + 2NaF + 3H_2O + H_2 \quad (1)$$

All reagents were of analytical purity and were used without further purification. In a typical experimental procedure, 2 g of NH_4F, 1 g of B_2O_3, and 3 g of Na were placed in a 20-mL stainless steel autoclave. The autoclave was tightly sealed, heated in an electric oven from room temperature to 700 °C with an increasing rate of 10 °C min^{-1}, and maintained at 700 °C for 30 h. After the autoclave was cooled to room temperature on standing, the raw product was collected and treated with absolute ethanol, dilute hydrochloric acid, and distilled water. The final product was then dried under vacuum at 60 °C for 10 h. The as-obtained product was labeled sample 1.

When the temperature was decreased to 500 °C, other experimental parameters being kept the same, the product was labeled sample 2.

The samples were characterized by powder XRD with Cu Kα radiation, FE-SEM (JSM-6700F), TEM (Hitachi-7000), and HRTEM (JEOL-2100). Thermogravimetric analysis (TGA) was performed on a Mettler Toledo TGA/SDTA 851 thermal analyzer. The optical absorption spectrum was measured with a UV–vis–NIR spectrometer (Shimadzu, UV-1700), and the photoluminescence (PL) properties were observed through a spectrofluorometer (ISSK2-Digital) at room temperature excited with a 200-nm laser beam.

Figure 1a shows a typical X-ray powder diffraction (XRD) pattern of sample 1. All the diffraction peaks could be indexed to h-BN, with lattice constants $a = 2.501$ Å and $c = 6.627$ Å, which are closed to the reported values (JCPDS card no. 34-0421: $a = 2.504$ Å, $c = 6.656$ Å). Figure 1b shows the typical XRD pattern of sample 2. The calculated lattice constants $a = 2.503$ Å and $c = 9.992$ Å are in good agreement with the reported values of r-BN (JCPDS card no. 45-1171). The strong

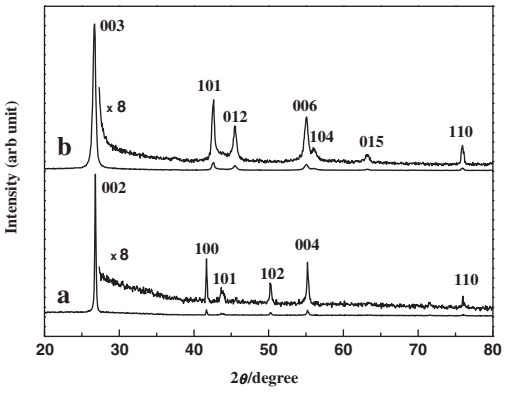

Figure 1. XRD patterns of the products: (a) sample 1 and (b) sample 2.

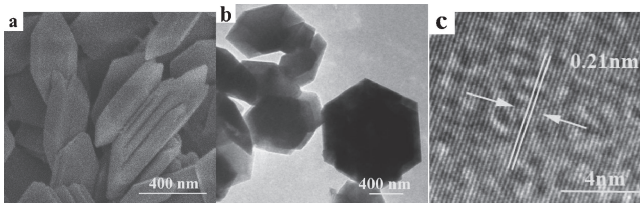

Figure 2. Typical SEM and HRTEM images of sample 1: (a) SEM image, (b) TEM image, and (c) HRTEM image obtained from part of an individual hexagonal nanoplate.

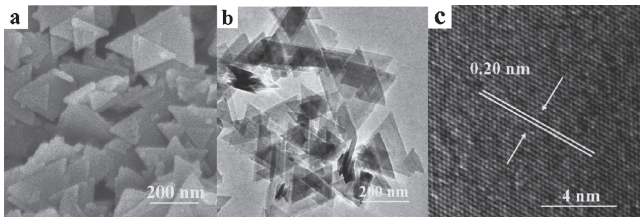

Figure 3. Typical SEM and HRTEM images of sample 2: (a) SEM image, (b) TEM image, and (c) HRTEM image obtained from part of an individual triangular nanoplate.

and sharp peaks indicated that sample 1 and sample 2 were highly crystalline. No other noticeable peaks of impurities were detected. In addition, from the different XRD patterns of sample 1 and sample 2, it can be seen that the (002) or (003) crystal plane has rather high diffraction intensity compared to other crystal planes, which indicates a strong preferred orientation in the samples. From the results of the XRD patterns of the two samples, it is confirmed that h-BN and r-BN were produced starting from NH_4F, B_2O_3, and Na.

Detailed morphology and structure analyses of the as-prepared samples were carried out by SEM and HRTEM. The typical SEM and HRTEM images of sample 1 are showed in Figure 2. The image shown in Figure 2a indicates that sample 1 is composed of a great amount of hexagonal nanoplates with smooth surface and uniform shapes, and the thickness is about 100 nm. Figure 2b shows the edge width of the hexagonal nanoplates ranges from 300 to 500 nm. A typical HRTEM image of the nanoplate (Figure 2c) shows the clearly resolved interfringe distances of 2.1 Å, which correspond to the (100) lattice spacing of h-BN. The results of the SEM and HRTEM images show that h-BN hexagonal nanoplates were formed when the temperature was 700 °C, which also confirms the preferential orientation of XRD patterns caused by the two-dimensional structures in the samples. Interestingly, when the temperature was decreased to 500 °C while the other conditions were kept constant, lots of triangular nanoplates were found. From the typical SEM image (Figure 3a) and TEM image (Figure 3b) of sample 2, one can found that sample 2 is composed of a large quantity of triangular nanoplates nearly 200 nm across and about 20 nm thick. Figure 3c gives the HRTEM image of sample 2 with the lattice spacing of about 2.0 Å, corresponding to (012) plane of r-BN.

The UV absorption spectra of the sample 1 (curve a) and sample 2 (curve b) are displayed in Figure 4. Two intense absorption bands centered at 206 and 204 nm are clearly observed for sample 1 and sample 2, respectively. The E_g

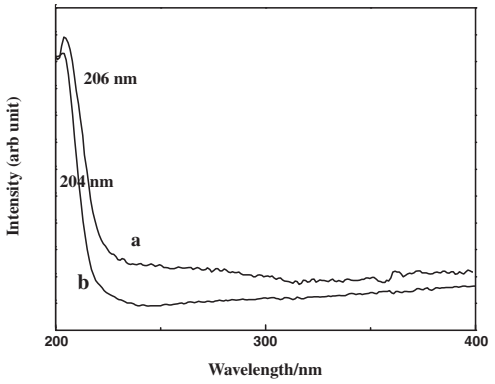

Figure 4. The UV absorption spectra of sample 1 (curve a) and sample 2 (curve b).

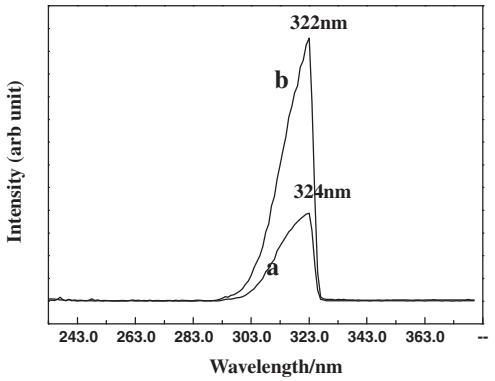

Figure 5. PL spectra of the product with excitation at 200 nm at room temperature: (a) sample 1 and (b) sample 2.

values of sample 1 and sample 2 are similar (about 6.04 eV), which is consistent with the previous report.[17] Furthermore, the PL spectra of sample 1 (Figure 5a) and sample 2 (Figure 5b) show intense emission peaks at 324 and 322 nm, respectively, which can be ascribed to structural defects,[18] such as nitrogen interstitials.[19] The UV and PL results proved that the products possess good optical properties, which can be used as promising materials for deep-blue and UV applications.

Figure 6a shows the thermal stability of the nanoplates analyzed by TGA in air. It was found that both samples have a small peak in the range of 40–360 °C, which can be attributed to the baseline drift of the TGA instrument (Figure 6b). Getting rid of the influence from the instrument, there is no significant change below 900 °C, which proved that the products are thermally more stable than previously reported.[14,15] As the temperature rose above 900 °C, the sample 2 showed a rather higher weight gain than sample 1, which proved thermal stability of h-BN hexagonal nanoplates was better than r-BN triangular nanoplates in air. The possible reasons are as follows: on the one hand, the phase of sample 1 has a smaller layer spacing and higher symmetry, which results in a more stable structure; on the other hand, sample 2 has much smaller particle size, which results in vulnerability to oxidation. Therefore, the h-BN nanoplates with great thermal stability and oxidation resistance may provide substantial applications in high-temperature electrooptical materials.

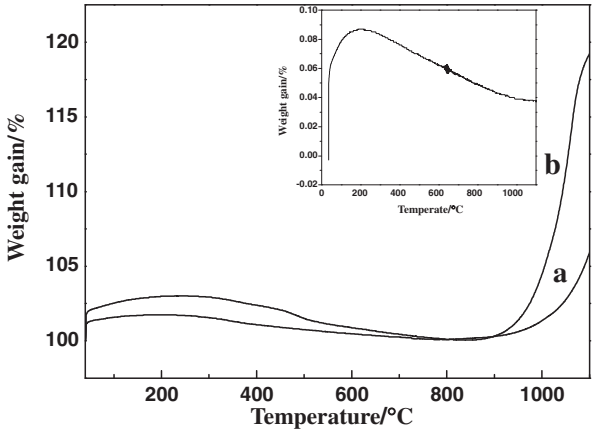

Figure 6. TGA curves of (a) sample 1 and (b) sample 2; inset is the TGA curve of the blank test.

In order to understand the effects of the reaction conditions on the formation of BN nanoplates, a series of experiments were conducted by changing the reaction temperature and reaction time. When the temperature was maintained at 700 °C for more than 10 h, the products were mainly h-BN hexagonal nanoplates. If the reaction time was less than 10 h, triangular and hexagonal nanoplates coexisted; hexagonal nanoplates gradually increased along with the extension of reaction time. When the temperature was maintained at 500–700 °C, while keeping other parameters constant, the samples are also mixtures of two forms. If the reaction temperature was 500 °C, amorphous BN was obtained after 1 h. When the reaction time was prolonged to 5 h, nanoplates with irregular shapes appeared. After 10 h of reaction, the product consisted of triangular nanoplates of smaller size. If the temperature was below 400 °C, almost no BN solid powder even amorphous one was collected.

In summary, crystalline h-BN hexagonal nanoplates were produced from B_2O_3, NH_4F, and Na at 700 °C for 30 h, and r-BN triangular nanoplates were obtained when the temperature was maintained at 500 °C with other conditions kept unchanged. TGA test results reveal that h-BN has superior thermal stability than that of r-BN even above 1000 °C, and the PL measurements indicate that both h-BN and r-BN have strong UV emission, which make the nanoplates good candidates for optical and optoelectronic devices.

This work was supported by the National Nature Science Foundation of China (Grant Nos. 20871075 and 20971079), the 973 Project of China (No. 2011CB935901), and the Independent Innovation Foundations of Shandong University (Nos. 2009TS017 and 2009JC019).

References

1 L. Liu, Y. P. Feng, Z. X. Shen, *Phys. Rev. B* **2003**, *68*, 104102.
2 K. Watanabe, T. Taniguchi, H. Kanda, *Nat. Mater.* **2004**, *3*, 404.
3 V. L. Y. Solozhenko, I. A. Petrusha, A. A. Svirid, *High Pressure Res.* **1996**, *15*, 95.
4 G. S. Oleinik, V. I. Lyashenko, *J. Superhard Mater.* **2008**, *30*, 287.
5 C. Tang, Y. Bando, T. Sato, K. Kurashima, *Chem. Commun.* **2002**, 1290.
6 T. Oku, K. Hiraga, T. Matsuda, T. Hirai, M. Hirabayashi, *Diamond Relat. Mater.* **2003**, *12*, 1138.
7 X. Wang, Y. Xie, Q. Guo, *Chem. Commun.* **2003**, 2688.
8 X. Hao, Y. Wu, J. Zhan, J. Yang, X. Xu, M. Jiang, *J. Phys. Chem. B* **2005**, *109*, 19188.
9 S. D. Yuan, X. X. Ding, Z. X. Huang, X. T. Huang, Z. W. Gan, C. Tang, S. R. Qi, *J. Cryst. Growth* **2003**, *256*, 67.
10 M. Li, L. Xu, L. Yang, Z. Bai, Y. Qian, *Diamond Relat. Mater.* **2009**, *18*, 1421.
11 M. Topsakal, E. Aktürk, S. Ciraci, *Phys. Rev. B* **2009**, *79*, 115442.
12 M. S. Si, D. S. Xue, *Phys. Rev. B* **2007**, *75*, 193409.
13 C. Tang, Y. Bando, D. Golberg, *Chem. Commun.* **2002**, 2826.
14 L. Q. Xu, J. H. Zhan, J. Q. Hu, Y. Bando, X. L. Yuan, T. Sekiguchi, M. Mitome, D. Golberg, *Adv. Mater.* **2007**, *19*, 2141.
15 M. Li, L. Xu, C. Sun, Z. Ju, Y. Qian, *J. Mater. Chem.* **2009**, *19*, 8086.
16 C. Zhi, Y. Bando, C. Tang, H. Kuwahara, D. Golberg, *Adv. Mater.* **2009**, *21*, 2889.
17 H. Chen, Y. Chen, Y. Liu, C.-N. Xu, J. S. Williams, *Opt. Mater.* **2007**, *29*, 1295.
18 M. G. Silly, P. Jaffrennou, J. Barjon, J.-S. Lauret, F. Ducastelle, A. Loiseau, E. Obraztsova, B. Attal-Tretout, E. Rosencher, *Phys. Rev. B* **2007**, *75*, 085205.
19 M. Fanciulli, T. D. Moustakas, *Physica B* **1993**, *185*, 228.

